Journal of Quantitative Spectroscopy & Radiative Transfer 112 (2011) 1250–1256

Contents lists available at ScienceDirect

Journal of Quantitative Spectroscopy & Radiative Transfer

journal homepage: www.elsevier.com/locate/jqsrt

Relevance of the subgrid-scales for large eddy simulations of turbulence–radiation interactions in a turbulent plane jet

M. Roger *, P.J. Coelho, C.B. da Silva

Mechanical Engineering Department, Instituto Superior Técnico/IDMEC, Technical University of Lisbon, Av. Rovisco Pais, 1049-001 Lisboa, Portugal

ARTICLE INFO

Available online 15 September 2010

Keywords:
Turbulence–radiation interaction
Subgrid-scales
Turbulent plane jet
Large eddy simulation
Radiative transfer
Direct numerical simulation

ABSTRACT

An *a priori* study based on direct numerical simulation (DNS) of a non-isothermal turbulent plane jet has been carried out in order to analyse the role of the small-scales of turbulence on thermal radiation. Filtered DNS and large eddy simulation (LES) without subgrid-scale (SGS) model have been estimated for the radiative heat transfer. The comparison of the results highlights the subgrid-scale influence over the filtered radiation quantities, such as the radiative intensity and the radiative emission. The influence of the optical thickness is also studied. It is shown that the subgrid-scales are not significant near the centerline of the jet, where the radiative heat transfer is more important, and therefore that the SGS can be neglected in this configuration. However, when the optical thickness increases, the SGS become relevant and SGS modeling may be needed.

© 2010 Elsevier Ltd. All rights reserved.

1. Introduction

Turbulence–radiation interaction (TRI) effects in reactive flows have been widely studied over the last years [1]. Direct numerical simulations (DNS) and large eddy simulations (LES) are the most accurate numerical techniques used for modeling turbulent flows [2]. DNS are frequently used to provide fundamental insight on turbulent flows and various studies have been carried out with DNS in recent years to investigate TRI [3–6]. But DNS remains too computational expensive for practical applications, and therefore LES emerges as an efficient approach with the increase of computational power for solving complex problems in combustion and fluid dynamics [7,8].

Thermal radiation has been coupled to LES of reactive flows in [9–13]. In these studies, the filtered radiative source term was estimated without subgrid-scale (SGS) models, *i.e.*, the influence of the LES unresolved scales over the radiative heat transfer has been neglected. Gupta et al. [13] have recently studied LES in a turbulent planar channel flow and analyse the influence of the LES resolved-scale TRI over the temperature, emission and absorption profiles. It is shown that the temperature self-correlation is the most important contributor to emission TRI, which is more significant than the absorption TRI, except at large optical thickness.

A few very recent works addressed the importance of SGS of thermal radiation in LES. The SGS-TRI in LES has been studied by Poitou et al. [14]. They performed a two-dimensional study from DNS of a reactive shear layer to evaluate the SGS-TRI in the emission of radiation and tested models based on Taylor development to reconstruct the correlation between the temperature and the absorption coefficient in a flame. Coelho [15] investigated the relevance of the SGS-TRI in Sandia flame D. He generated a time-series of turbulent scalar fluctuations along optical paths of the flame and solved the filtered radiative transfer equation (RTE) along these paths by applying a one-dimensional filtering operation. In this study, various approximations based on an assumed

* Corresponding author. Tel.: +351 21 841 81 94; fax: +351 21 847 55 45.
E-mail address: roger.maxime@ist.utl.pt (M. Roger).

0022-4073/$ - see front matter © 2010 Elsevier Ltd. All rights reserved.
doi:10.1016/j.jqsrt.2010.08.026

subgrid-scale probability density function are tested to model the subgrid-scale fluctuations of thermal radiation. It is shown that the TRI in LES is less relevant than in RANS calculations, and that an extension of the optical thin fluctuation approximation (OTFA) to LES should be adequate. In the study of Chandy et al. [16], a hybrid LES/filtered mass density function (FMDF) has been applied to simulate a turbulent sooty flame. The extension of the OTFA was used for the SGS absorption TRI, and the closure of the filtered emission term is done by the statistics of the composition variables available in the context of LES/FMDF. It is shown that ignoring SGS-TRI emission increases the overall temperature of the flame, by decreasing the radiative heat loss.

A rigorous evaluation of the role of the SGS-TRI in LES requires DNS data. In our previous studies [17,18], the influence of the SGS over the radiative heat transfer has been studied in an analysis based on DNS of steady forced homogeneous isotropic turbulence. This analysis assessed the relevant terms of the filtered radiative transfer equation (FRTE). It has been shown in [17] that the influence of the SGS-TRI over the radiative absorption can be neglected whereas the influence over the emission term may need to be taken into account in some configurations, namely when the temperature standard deviation reaches 20% of the mean temperature and the filter size is located in the low-inertial range of the kinetic energy spectrum. In [18], the influence of the mean and variance temperature on the subgrid-scale correlations is studied. It is shown that the assumption of neglecting the TRI in LES leads to good predictions in the tested cases.

With the aim of including radiative heat transfer calculations in a LES code of turbulent non-premixed jet flames, this study extends our preceding analysis to a turbulent jet configuration. A DNS code of a non-isothermal turbulent plane jet is used, and the radiative transfer calculations are decoupled from the DNS. Combustion is not taken into account in this study and will be the subject of future works. Even if this configuration remains academic, the flow studied here is representative of jets, wakes and mixing layers [19], and displays some universal qualitative features related to the entrainment in free shear flows.

In the present work, DNS, filtered DNS and LES without SGS model have been carried out in order to study the influence of the SGS over the thermal radiation. The main contribution lies in the *a priori* analysis based on simultaneous filtered DNS and LES without SGS model calculations to investigate the role of LES-SGS on radiative quantities based on DNS data of a turbulent plane jet. Previous works were limited to filtered DNS tests [14,17], applied in homogeneous isotropic turbulence configuration [17,18], relied on a stochastic model rather than DNS [15] or focused on the role of TRI in RANS based on DNS [3,6,5] or LES [13]. DNS resolves all the turbulent scales, until the smallest active ones. Comparing filtered DNS and LES estimates in an *a priori* analysis allows to identify the effect of the LES-SGS over the radiative quantities. The influence of the optical thickness is also investigated.

2. Jet modeling

2.1. DNS of a turbulent plane jet

The present work is based on a direct numerical simulation (DNS) of a turbulent planar jet described in [20]. The turbulent plane jet is a well known canonical free shear flow with many common features with other free shear flows, such as mixing layers, wakes, round and coaxial jets. Therefore it is expected that the results described here are similar to the results obtained in other free shear flows.

In a jet produced in a laboratory setup, the jet spreads freely from an initial source of momentum into a tank filled with the same fluid at rest. Spatial DNS of jets describe the jets observed in the laboratory as sketched in Fig. 1(a). However, it is well known that numerical simulations of spatially developing flows such as jets can be very demanding both in terms of computer time and memory, due to the need to simulate the flow inside a very large computational domain containing all the length

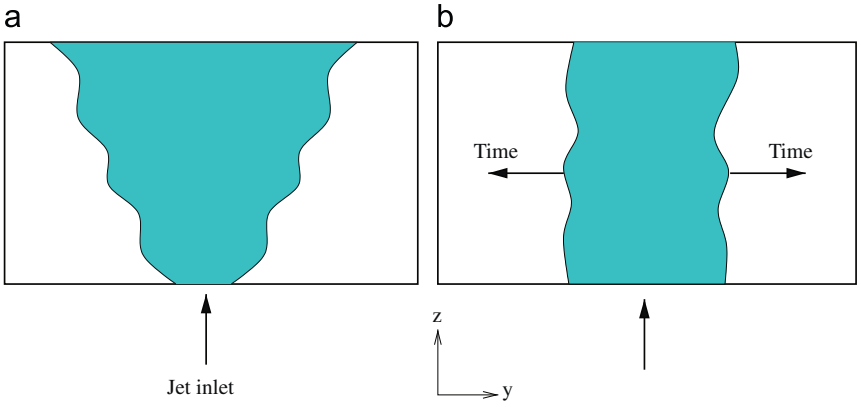

Fig. 1. Sketch of (a) a spatially developing jet as produced in a laboratory setup and (b) a temporal jet simulation as the one adopted in the present work.

scales of the flow. Recent DNS of spatially evolving turbulent plane jets include the works of Stanley et al. [21] and da Silva et al. [22]. In the present work in order to limit the computational cost we use temporal simulations, where the streamwise direction is periodic and we analyse the spreading rate of the shear layer in time as sketched in Fig. 1(b). This roughly corresponds to analysing the spatial developing jet through a moving window that travels downstream with the local mean speed of the jet. The temporal simulation approach is particularly suited to study the far field of the jet in great detail since the number of available points in this region is maximized in temporal simulations [20]. Moreover the temporal simulation approach permits the use of the very fast and accurate pseudo-spectral methods. DNS of temporally evolving turbulent plane jets were carried out by Akhavan et al. [23] and da Silva et al. [19].

The Navier–Stokes equations and an equation for the transport of a passive scalar field were solved in the temporal plane jet configuration. The numerical code used here employs pseudo-spectral schemes for spatial discretization and the temporal advancement is made with an explicit third order Runge–Kutta time stepping scheme. More details can be found in [20]. The grid size uses $(N_x,N_y,N_z)=(256,384,256)$ grid points along the spanwise (x), the lateral (y) and streamwise z directions, respectively, and the dimension of the computational domain is equal to $L_x=L_z=4H$ and $L_y=6H$, where H is the inlet slot-width of the jet. The initial Reynolds number is $Re_H = U_0H/\nu = 3200$, where ν is the kinematic viscosity. The initial condition consists of a mean velocity profile to which a synthetic numerical noise was added [20]. The mean initial velocity used here consists on a hyperbolic-tangent velocity profile,

$$U_0(x,y,z) = \frac{1}{2} - \frac{1}{2}\tanh\left[\frac{H}{4\theta_0}\left(1 - \frac{2|y|}{H} - \frac{|y_0|}{H}\right)\right] \quad (1)$$

where θ_0 is the initial momentum thickness. Notice that in this work the jet centerline is located at $y_0/H=3$. Many temporal simulations of turbulent round jets use a similar initial mean velocity profile, since it is recognized that it represents a very good approximation to the inlet velocity profile found in measured experimental jets [24]. The passive scalar field was initialized with a similar mean profile to which no initial passive scalar noise was added.

Due to the nature of the temporal simulations, mixed spatial–temporal means are used to obtain the statistics as described in [20]. The spatial means consists in averaging along the $N_x \times N_z$ homogeneous directions, while temporal averaging is done with 14 instantaneous fields from the far-field self-similar regime. Furthermore, symmetry along the N_y direction is used. In total, each mean quantity is estimated from $256 \times 256 \times 2 \times 14 \simeq 1.8 \times 10^6$ samples, which ensures a good convergence of the statistics.

2.2. Temperature and gas species concentration data

In order to generate the temperature and the species concentration fields for the radiative transfer computations, we use the passive scalar fields obtained from the above DNS. The Prandtl number is equal to 0.7. Since the plane jet is homogeneous in the spanwise (x) and streamwise (z) directions, the statistical moments of the temperature and of the species concentration depend only on the lateral direction (y). At each plane (x,z) (defined by y constant), the instantaneous temperature field has been determined from the passive scalar field according to the following expression [17]:

$$T(x,y,z) = \langle T\rangle(y) + [T_{DNS}(x,y,z) - \langle T_{DNS}\rangle(y)]\sqrt{\frac{\langle T'^2\rangle(y)\rangle}{\langle T_{DNS}{}'^2\rangle(y)\rangle}} \quad (2)$$

In this expression, $\langle T\rangle$ is the mean temperature and $\langle T'^2\rangle$ is the variance of the temperature in the plane (x,z). $T_{DNS}(x,y,z)$ is the value of the instantaneous passive scalar field, $\langle T_{DNS}\rangle$ and $\langle T_{DNS}{}'^2\rangle$ are its mean and variance, respectively. The first and second statistical moments of the temperature are obtained from the first and second moments of the passive scalar field according to the following linear expression:

$$\langle T\rangle(y) = \langle T\rangle_{min} + \frac{\langle T_{DNS}\rangle(y) - \langle T_{DNS}\rangle_{min}}{\langle T_{DNS}\rangle_{max} - \langle T_{DNS}\rangle_{min}} \times (\langle T\rangle_{max} - \langle T\rangle_{min}) \quad (3)$$

$$\sqrt{\langle T'^2\rangle}(y) = \sqrt{\langle T'^2\rangle}_{min} + \frac{\sqrt{\langle T'^2_{DNS}\rangle}(y) - \sqrt{\langle T'^2_{DNS}\rangle}_{min}}{\sqrt{\langle T'^2_{DNS}\rangle}_{max} - \sqrt{\langle T'^2_{DNS}\rangle}_{min}} \times \left(\sqrt{\langle T'^2\rangle}_{max} - \sqrt{\langle T'^2\rangle}_{min}\right) \quad (4)$$

Similar expressions for the CO_2 molar fraction field are obtained, since it was supposed that the temperature and the absorbing species are fully correlated [17]. This assumption is consistent with an infinitely fast chemistry model and it is widely used in combustion modeling, provided that local extinction and reignition are not significant. The conserved scalar/prescribed pdf formulation for example relies on the assumption of such a correlation [25].

The time-averaged temperature $\langle T\rangle$ profile is displayed in Fig. 2 and an example of an instantaneous temperature

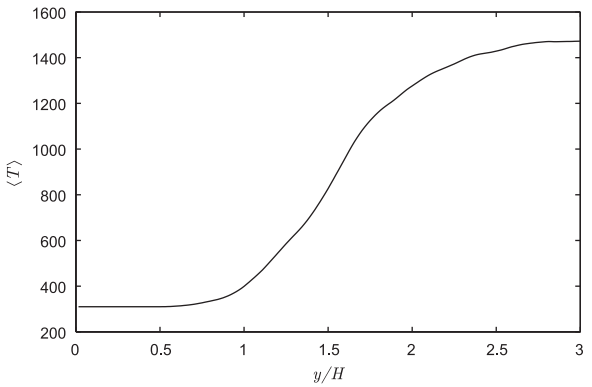

Fig. 2. Time-averaged temperature $\langle T\rangle$ (in K) profile of the jet along the (y) direction.

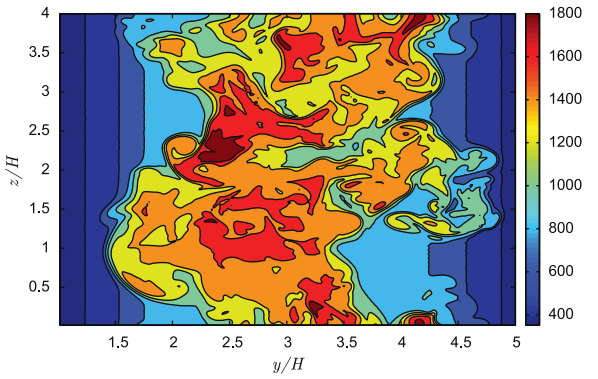

Fig. 3. Example of instantaneous temperature (in K) in a (y,z) plane chosen arbitrarily.

field in a (y,z) plane is presented in Fig. 3. It can be observed that the flow is strongly anisotropic along the y direction.

3. Thermal radiation calculations

The radiative transfer calculations have been carried out using a ray tracing/correlated-k distribution method, as described in [17]. Although radiation from H_2O can be easily included in the calculations, only radiation from CO_2 is considered in order to reduce the computational requirements. The ray-tracing method consists in solving the RTE along a line of sight in its integral form, which may be written as

$$I_\nu(s) = I_\nu(0)\exp\left(-\int_0^s \kappa_\nu(s')\,ds'\right) + \int_0^s \kappa_\nu(s')I_{b\nu}(s')\exp\left(-\int_{s'}^s \kappa_\nu(s'')\,ds''\right)ds' \quad (5)$$

Eq. (5) has been discretized by dividing the optical path into elements and interpolating the temperature and chemical composition using cubic splines. The integrals in Eq. (5) are numerically evaluated using Simpson's rule, to guarantee that the order of accuracy in the evaluation of the radiation intensity is similar to that of DNS. The integration over the spectrum has been done using the correlated-k distribution method (CK approximation) [26]. The parameters needed for the CK approximation are taken from the data of Soufiani and Taine [27]. In the DNS and in the filtered DNS tests, the RTE is solved directly in the DNS grid. The interpolations using cubic splines are applied on the temperature and CO_2 species molar fraction fields. In the LES, the RTE is solved in a coarser grid, and the interpolations are applied on the filtered temperature, $\overline{T}$, and CO_2 molar fraction, $\overline{X}_{CO_2}$, fields.

For the filtered DNS estimations, the RTE is solved at all the scales of motion in the DNS grid, and the radiative quantities obtained, such as the radiation intensity and the emission, are filtered by a box filter of size Δ. The filtered radiative intensity is denoted by $\overline{I}_{DNS}$. It is then possible to obtain all the filtered reference quantities in which the role of the SGS-TRI is taken into account. Three different filter sizes have been tested in this study: $\Delta = m\delta$ with $m \in \{4,8,16\}$, where δ is the DNS grid size. The filter size equal to 4δ is located in the dissipation range of the kinetic energy spectrum, while the filter sizes equal to 8δ and 16δ are located in the inertial range of the spectrum. It should be noted that the two last filter sizes are the most representative of the filter sizes used in practical LES applications.

The filtered RTE (FRTE) can be written as

$$\frac{d\overline{I}_\nu}{ds} = -\overline{\kappa_\nu I_\nu} + \overline{\kappa_\nu I_{b\nu}} \quad (6)$$

In the LES tests, the grid itself acts as a filter for the calculations and the SGS-TRI has been neglected. In this case, the FRTE takes the following form:

$$\frac{d\overline{I}_\nu}{ds} \simeq -\overline{\kappa}_\nu \overline{I}_\nu + \overline{\kappa}_\nu \overline{I}_{b\nu} \quad (7)$$

It is further assumed that $\overline{I}_{b\nu} \simeq I_{b\nu}(\overline{T})$ and $\overline{\kappa}_\nu \simeq \kappa_\nu(\overline{T},\overline{X}_{CO_2},\overline{X}_{H_2O})$, *i.e.*, the temperature self-correlation is neglected as well as the correlation between the absorption coefficient and the temperature/chemical composition. The total filtered radiation intensity obtained from Eq. (7) is expressed as $\overline{I}_{LES}$. The same filter sizes as used in the filtered DNS estimations are applied, *i.e.*, $\Delta = m\delta$ with $m \in \{4,8,16\}$.

4. Results

The standard conditions used for the radiative transfer calculations are chosen such that the maximum time-averaged temperature in the normal direction is $\langle T \rangle_{max} = 1500\,\mathrm{K}$ and the maximum temperature standard deviation is equal to $\sqrt{\langle T'^2 \rangle}_{max} = 300\,\mathrm{K}$. Far away from the jet centerline, where there is no turbulence, the minimum values for the averaged temperature and standard deviation are $\langle T \rangle_{min} = 310\,\mathrm{K}$ and $\sqrt{\langle T'^2 \rangle}_{min} = 0$. The mean molar fraction of CO_2 varies between 0.1 and 0.5 and the maximum molar fraction standard deviation is $\sqrt{\langle X'^2_{CO_2} \rangle}_{max} = 0.1$.

4.1. Influence of the subgrid-scale fluctuations over the radiative intensity

In Fig. 4 the time-averaged radiation intensity calculated from DNS data along the (y) direction is displayed. The optical thickness τ estimated by $\langle \kappa_P \rangle_{y=3H} \times L_y$ is equal to 10. The maximum mean radiative intensity is located slightly after the centerline of the jet (which is located at y/H=3) at this optical thickness, as expected from calculations carried out along radial lines of sight of free jet diffusion flames, which exhibit qualitatively similar temperature and absorbing species profiles [15]. In Fig. 4, the mean filtered radiative intensities obtained from the DNS and the *a priori* calculations are displayed for various filter sizes. As expected, in the case of a filter size located in the dissipation range ($\Delta = 4\delta$), the results are very close to those determined from DNS. The difference between $\langle \overline{I}_{DNS} \rangle$ and $\langle \overline{I}_{LES} \rangle$ remains small when $\Delta = 8\delta$. This confirms the statement made in the

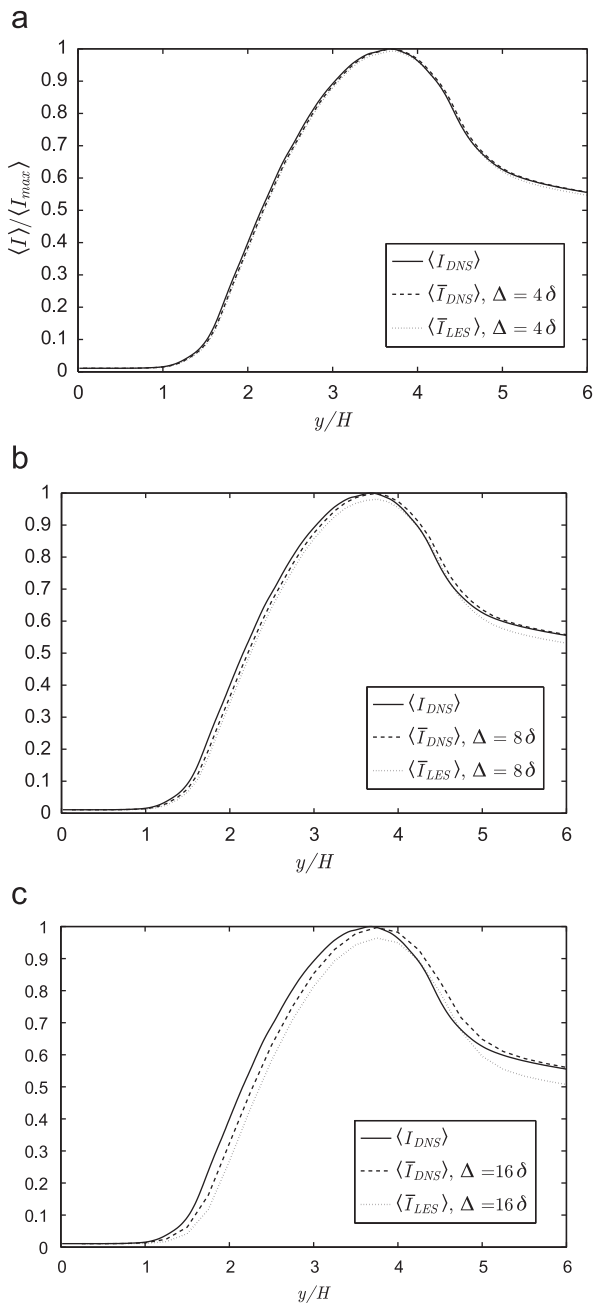

Fig. 4. Time-averaged normalized filtered radiation intensity $\langle \overline{I}\rangle/\langle I\rangle_{max}$ along the (y) direction estimated with $\Delta = 4\delta$ (a), $\Delta = 8\delta$ (b) and $\Delta = 16\delta$ (c).

studies [15,17] that the subgrid-scale TRI influence can be neglected in various configurations. However, that difference becomes significant in the case $\Delta = 16\delta$. It can be observed for this filter size that $\langle \overline{I}_{LES}\rangle$ is lower than $\langle \overline{I}_{DNS}\rangle$, which means that the overall subgrid-scale TRI increases the radiation intensity.

In Fig. 5, the results concerning the radiative emission are presented. Only half of the domain is shown due to symmetry. The radiative emission estimated from filtered

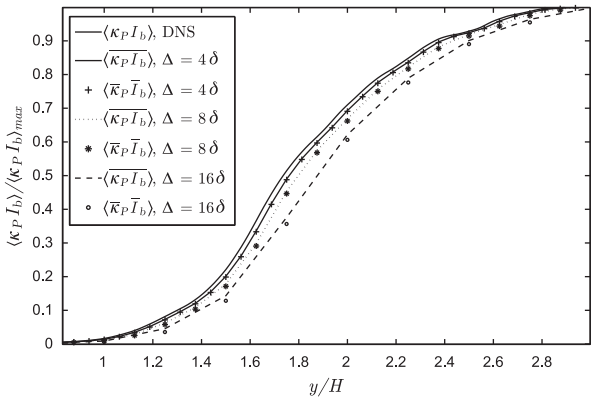

Fig. 5. Time-averaged normalized radiative emission $\langle \kappa_P I_b\rangle/\langle \kappa_P I_b\rangle_{max}$ along the (y) direction, estimated from DNS, filtered DNS and LES calculations.

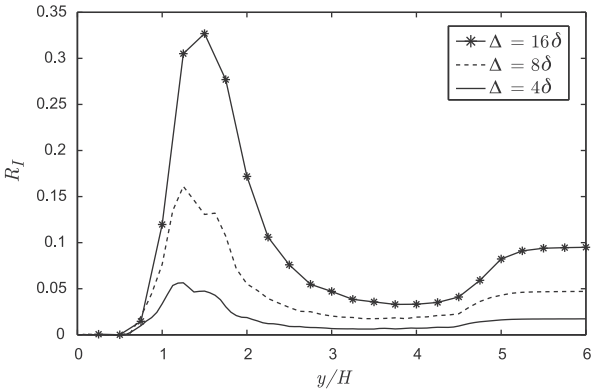

Fig. 6. Ratio of the subgrid-scale over the grid-scale radiative intensity.

DNS is denoted by $\overline{\kappa_P I_b}$ while that from LES computations is identified as $\overline{\kappa}_P \overline{I}_b$. We recall that all the subgrid-scale correlations have been neglected in the LES tests, thus it is assumed that $\overline{\kappa}_P \simeq \kappa_P(\overline{T}, \overline{X}_{CO_2})$ and $\overline{I}_b \simeq I_b(\overline{T})$. Therefore, the difference between $\langle \overline{\kappa_P I_b}\rangle$ and $\langle \overline{\kappa}_P \overline{I}_b\rangle$ is the consequence of the overall SGS emission TRI. It can be seen that the profiles are almost merged in the cases $\Delta = 4$ and 8δ, while in the case $\Delta = 16\delta$ the profiles remain very close.

In order to evaluate the relative SGS influence in comparison with the resolved-scale (grid-scale), the following ratio is introduced:

$$R_I = \frac{\langle \overline{I}_{DNS} - \overline{I}_{LES}\rangle}{\langle \overline{I}_{DNS}\rangle} \tag{8}$$

R_I represents the influence of the SGS-TRI, estimated by $(\overline{I}_{DNS} - \overline{I}_{LES})$ over the grid-scale radiative intensity $\overline{I}_{DNS}$. Fig. 6 displays the value of this ratio for the three studied filter sizes. R_I reaches relatively high values of about 30% for $\Delta = 16\delta$ near the jet edge, where the mean temperature gradients are high, *i.e.*, for $y/H \in [0.5,2]$. However, this significant influence of the SGS is restricted to the zone where the radiation intensity is small (see Fig. 4). In the central zone, where the temperature is highest, the

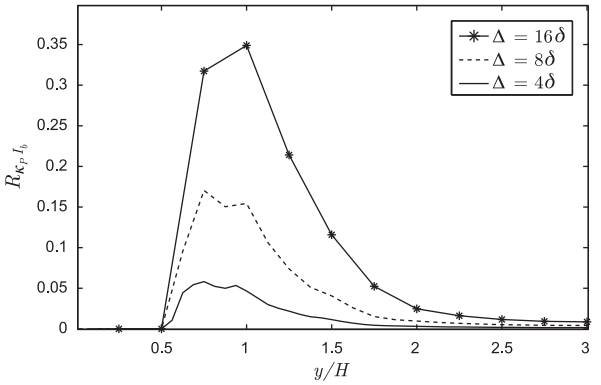

Fig. 7. Ratio of the subgrid-scale over the grid-scale radiative emission.

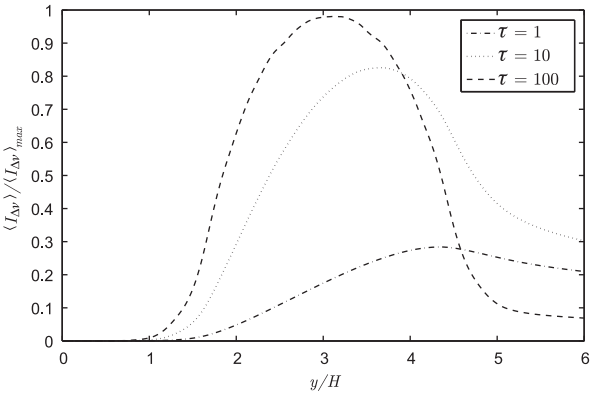

Fig. 8. Time-averaged normalized band-averaged radiative intensity $\langle I_{\Delta\nu}\rangle/\langle I\rangle_{max}$ along the (y) direction, estimated from DNS.

SGS-TRI is much smaller (5% in the center of the jet at y=3H for $\Delta = 16\delta$). Similarly, the following ratio is introduced for the radiative emission:

$$R_{\kappa_P I_b} = \frac{\langle \overline{\kappa_P I_b} - \overline{\kappa}_P \overline{I}_b \rangle}{\langle \overline{\kappa_P I_b} \rangle} \tag{9}$$

In this case, $R_{\kappa_P I_b}$ represents the influence of the SGS emission TRI over the resolved emission. The same observation as for R_I can be made in Fig. 7, *i.e.*, the influence of the SGS is significant near the jet edge. This means that for the considered optical thickness, the SGS emission TRI is only significant in the zone where the radiative transfer is less important, and can therefore be neglected.

The evaluation of the influence of SGS-TRI on the radiative absorption is not investigated in this study, because previous works [15,17,18] shown that its role is small in comparison with the radiative emission.

4.2. Influence of the optical thickness

The influence of the optical thickness is now investigated. The calculations have been carried out in a single band in order to decrease the computational cost. The band chosen is the strongest absorption band of the CO_2 spectrum, defined by the wavenumbers [2250,2400] (cm^{-1}). The estimated band-averaged radiative intensity is equal to $I_{\Delta\nu} = \sum_{j=1}^{N_Q} \omega_j I_{\Delta\nu,j} \Delta\nu$, where the ω_j are quadrature weights and N_Q is the number of quadrature points.

In Fig. 8, the normalized band-averaged radiative intensity is displayed for three optical thicknesses $\tau = 1$, 10 and 100. τ is defined as the product of the mean absorption coefficient in the band by L_y. At the large optical thickness of $\tau = 100$, the profile of $\langle I_{\Delta\nu}\rangle$ is similar to the temperature profile, because the emitted radiation is absorbed locally close to the point of emission, and the symmetry of the jet is observed. In Fig. 9, the calculations for $\Delta = 8\delta$ are displayed. It can be seen that the profiles of $\overline{I}_{LES}$ and $\overline{I}_{DNS}$ are almost merged at small and intermediate optical thickness ($\tau = 1$ and 10). For $\tau = 100$, a difference is observed, especially at the zone of the flow where

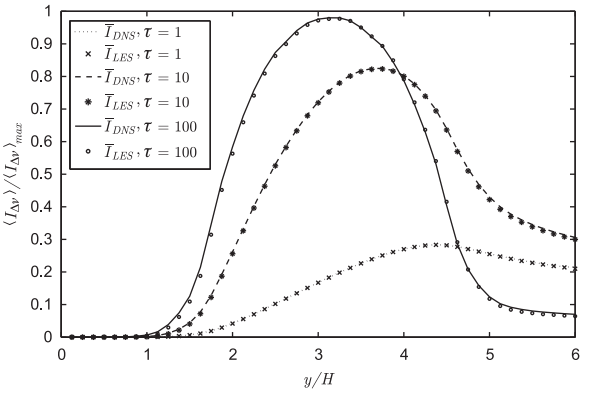

Fig. 9. Time-averaged normalized band-averaged filtered radiative intensity $\langle \overline{I}_{\Delta\nu}\rangle/\langle I\rangle_{max}$ along the (y) direction for $\Delta = 8\delta$.

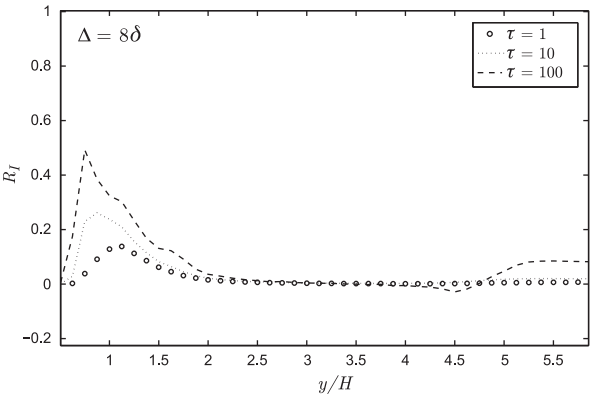

Fig. 10. Ratio of the subgrid-scale over the grid-scale band-averaged radiative intensity for different optical thicknesses.

the temperature variance is highest. In those cases, the SGS-TRI may have an influence on the resolved radiation.

The profiles of R_I, calculated from Eq. (8) using the band-averaged rather than the total radiation intensity, and estimated with $\Delta = 8\delta$ are presented in Fig. 10. The relative influence of the SGS over the resolved radiative intensity is significant near the jet edge, *i.e.*, $y/H \in$ [0.5,2]

and $y/H \in [4,5.5]$. This feature of the SGS at this zone of the flow had already been observed for many other flow variables [28]. However, in the zone where the radiative heat transfer is more important, the influence of the SGS remains small, as observed above.

5. Conclusion

In this study, DNS of a turbulent plane jet has been carried out along with the resolution of the RTE in order to analyse the influence of the turbulent subgrid-scales upon LES of thermal radiation. The objective is to guide the coupling of radiative heat transfer in a LES code of turbulent jet flames. Filtered DNS and LES without SGS model have been applied to radiative transfer in an *a priori* analysis. It is shown that the relative influence of the SGS is important near the jet edge, where the mean temperature gradient is large. But the radiative transfer is small in this zone, which confirms the results of previous studies [15,17,18], which stated that neglecting the SGS-TRI may be valid in various cases. However, this assumption should be taken carefully when the optical thickness becomes large.

The number of simplifications made in this study implies that the extrapolation of the results to the jet flame region should be cautious. The flow considered is non-reactive, and consequently this study is relevant at the far field of a jet flame. The radiative transfer calculations have been decoupled from the DNS. Moreover, the influence of the subgrid-scales may be higher if the turbulence intensity increases, like in the near field of the jet nozzle, or with a higher Reynolds number. The present work is a contribute to our main objective which is to couple the radiative heat transfer in a LES code of a turbulent jet flame, work which is presently in progress.

Acknowledgement

Financial support of FCT-Fundação para a Ciência e a Tecnologia within the framework of project PDTC/EME-MFE/102405/2008 is acknowledged.

References

[1] Coelho P. Numerical simulation of the interaction between turbulence and radiation in reactive flows. Prog Energy Combust Sci 2007;33(4):311–84.
[2] Pope S. Turbulent flows. Cambridge University Press; 2000.
[3] Wu Y, Haworth D, Modest M, Cuenot B. Direct numerical simulation of turbulence/radiation interaction in premixed combustion systems. Proc Combust Inst 2005;30(1):639–46.
[4] Deshmukh K, Haworth D, Modest M. Direct numerical simulation of turbulence–radiation interactions in homogeneous nonpremixed combustion systems. Proc Combust Inst 2007;31(1):1641–8.
[5] Deshmukh K, Modest M, Haworth D. Direct numerical simulation of turbulence–radiation interactions in a statistically one-dimensional nonpremixed system. J Quant Spectrosc Radiat Transf 2008;109(14):2391–400.
[6] da Silva C, Malico I, Coelho P. Radiation statistics in homogeneous isotropic turbulence. New J Phys 2009;11 093001-34.
[7] Janicka J, Sadiki A. Large eddy simulation of turbulent combustion systems. Proc Combust Inst 2005;30(1):537–47.
[8] Pitsch H. Large-eddy simulation of turbulent combustion. Annu Rev Fluid Mech 2006;38:453–82.
[9] Desjardin P, Frankel S. Two-dimensional large eddy simulation of soot formation in the near-field of a strongly radiating non-premixed acetylene-air turbulent jet flame. Combust Flame 1999;119(1–2):121–32.
[10] Haworth D, Singh V, Gupta A, Modest M. Large eddy simulation of turbulent flows with thermal radiation and turbulence/radiation interaction. In: 58th Annual meeting of the American Physical Society Division of Fluid Dynamics, 2005.
[11] Jones W, Paul M. Combination of DOM with LES in a gas turbine combustor. Int J Eng Sci 2005;43(5–6):379–97.
[12] dos Santos RG, Lecanu M, Ducruix S, Gicquel O, Diacona E, Veynante D. Coupled large eddy simulations of turbulent combustion and radiative heat transfer. Combust Flame 2008;152(3):387–400.
[13] Gupta A, Modest M, Haworth D. Large-eddy-simulation of turbulence–radiation interactions in a turbulent planar channel flow. J Heat Transf 2009;131 (061704).
[14] Poitou D, Hafi ME, Cuenot B. Diagnosis of turbulence radiation interaction in turbulent flames and implications for modeling in large eddy simulation. Turkish J Eng Environ Sci 2007;31(6):371–81.
[15] Coelho P. Approximate solutions of the filtered radiative transfer equation in large eddy simulations of turbulent reactive flows. Combust Flame 2009;156(5):1099–110.
[16] Chandy A, Glaze D, Frankel S. A hybrid large eddy simulation/filtered mass density function for the calculation of strongly radiating turbulent flames. J Heat Transf 131 (051201).
[17] Roger M, da Silva C, Coelho P. Analysis of the turbulence–radiation interactions for large eddy simulation of turbulent flows. Int J Heat Mass Transf 2009;52(9–10):2243–54.
[18] Roger M, Coelho P, da Silva C. The influence of the non-resolved scales of thermal radiation in large eddy simulation of turbulent flows: a fundamental study. Int J Heat Mass Transfer 2010;53(13–14):2897–907.
[19] da Silva C, Pereira J. The effect of subgrid-scale models on the vortices computed from large eddy simulations. Phys Fluids 2004;16:4506–34.
[20] da Silva C, Pereira J. Invariants of the velocity-gradient, rate-of-strain, and rate-of-rotation tensors across the turbulent/nonturbulent interface in jets. Phys Fluids 2008;20:055101.
[21] Stanley S, Sarkar S, Mellado JP. A study of the flowfield evolution and mixing in a planar turbulent jet using direct numerical simulation. J Fluid Mech 2002;450:377–407.
[22] da Silva CB, Métais O. On the influence of coherent structures upon interscale interactions in turbulent plane jets. J Fluid Mech 2002;473:103–45.
[23] Akhavan R, Ansari A, Kang S, Mangiavacchi N. Subgrid-scale interactions in a numerically simulated planar turbulent jet and implications for modelling. J Fluid Mech 2000;408:83–120.
[24] Freymuth P. On transition in a separated laminar boundary layer. J Fluid Mech 1966;25:683.
[25] Peters N. Turbulent combustion. Cambridge University Press; 2000.
[26] Goody R, West R, Chen L, Crisp D. The correlated-k method for radiation calculations in non-homogeneous atmospheres. J Quant Spectrosc Radiat Transf 1989;42(6):539–50.
[27] Soufiani A, Taine J. High temperature gas radiative property parameters of statistical narrow-band model for H_2O, CO_2 and CO, and correlated-K model for H_2O and CO_2. Int J Heat Mass Transf 1997;40(4):987–91.
[28] da Silva C. The behavior of subgrid-scale models near the turbulent/nonturbulent interface in jets. Phys Fluids 2009;21:081702.